Side-Chain Liquid Crystalline Block Copolymers with Well Defined Structures Prepared by Living Anionic Polymerization IV. Microphase Morphology in Blends with Coil Homopolystyrenes

Tomomichi Itoh,* Naoki Tomikawa,* Masayuki Yamada,* Masatoshi Tokita,*
Akira Hirao,* and Junji Watanabe*,**,†

*Department of Polymer Chemistry, Tokyo Institute of Technology, Ookayama,
Meguro-ku, Tokyo 152–8552, Japan
**CREST-JST (Japan Science and Technology Corporation), 4–1–8 Hon-cho,
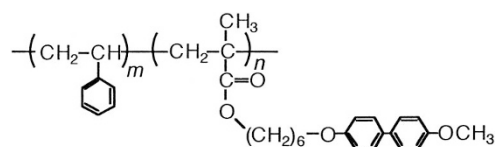Kawaguchi, Saitama 332–0012, Japan

ABSTRACT: The microdomain structure in the blends of liquid crystal (LC)-coil block copolymer with coil homopolymers was studied. The LC-coil block copolymer used is composed of poly(6-[4-(4′-methoxyphenyl) phenoxy] hexyl methacrylate) as a LC segment and polystyrene as a coil segment. It has the molecular weight $M_n = 47000$ with the LC segment fraction of 45 wt%. As a coil homopolymer, three polystyrenes with different molecular weights of 37000, 26000, and 8200 were used. In all the blends with LC segment fractions of 35% to 10%, the microphase segregation is clearly recognized and LC segment in resulting microdomain undergoes the well defined crystal-SmA-isotropic phase transitions. The microdomain structure depends on both the molecular weight of homopolystyrene blended and the phase structure of LC segment. When the highest molecular weight polystyrene with $M_n = 37000$ was blended (so called in a "dry-brush" regime), a lamellar type of morphology is invariably observed even if the composition and temperature are varied. In contrast, when the lowest molecular weight polystyrene with $M_n = 8200$ was used (in a "wet-brush" regime), the type of morphology is significantly altered. At the isotropic temperatures of LC segment, the lamellar morphology is observed for the blends with LC contents from 45% to 35%, but the cylindrical or spherical domain becomes predominant with a decrease in the LC content. On the other hand, the lamellar morphology is commonly observed at the crystal temperatures. In some blends with the lower weight fractions of LC segment, hence, there can be seen the order–order transition from sphere or cylinder to lamella on decreasing temperature. This morphological transformation is caused by the formation of the layered structure that tends to orient perpendicularly to the interface of microdomain. The results show that the structural order of LC segment affects both the microdomain morphology and the solubility style of the homopolymer into the block copolymer.

KEY WORDS   Side-Chain Liquid Crystalline Polymer / Block Copolymer / Blend / Morphology / Microphase Separation / Order–Order Transition /

In recent years, many researchers have been interested in the liquid crystal (LC)-coil block copolymer systems.[1–8] These LC block copolymers have two different ordering structures, microdomain structure and LC phase structure. In other words, the LC molecules have to undergo the phase transitions in a restricted space of the microdomain with the various sizes and shapes. Hence, when they form the highly anisotropic microstructure in the liquid crystal and crystal, the morphology may be altered from that in the isotropic phase. Conversely, if the microdomain morphology is tightly maintained, the transition behavior of the LC segment may be strongly affected. To clarify this relationship between two different ordering structures is one of the interesting subjects in the polymer liquid crystal field.

In previous studies,[9–11] we prepared the block copolymers (PS-*b*-poly(*lc*)s) composed of polystyrene (abbreviated here PS) and LC poly(6-[4-(4′-methoxy-

phenyl) phenoxy] hexyl methacrylate) (abbreviated poly(*lc*)) segments by a sequential anionic living polymerization. All the block copolymers with various molecular weights and segment compositions of around 50 wt% exhibited the lamellar type of segregation and their poly(*lc*) segments formed crystal, smectic A (SmA) and isotropic phases like in the homopoly(*lc*). The layered structures of crystal and SmA were formed with the side-chain mesogens lying parallel to the microdomain interface, *i.e.*, with the layers lying perpendicular to the interface. Most interesting is that the lamellar thickness is dependent on the SmA temperature (see later Figure 3). With increasing temperature, it decreased continuously from the value in the crystalline

---

†To whom correspondence should be addressed.

phase to that of isotropic phase; no jump could be seen on both the crystal-SmA and SmA-isotropic transitions. The overall change was completely reversible on heating and cooling cycles, indicating that it proceeds at a thermodynamic equilibrium. The reduction was about 20–25%, which is associated with the conformational change in the main chain of LC segment from the extended form in the crystalline phase to the random coil in the isotropic phase. Such a conformational change was considered to arise as a result of the counterbalance between conformational entropy gain of the main chain and energetic cost due to the layer ordering of the side-chain mesogens.

Several other types of microdomains, cylinder, sphere and bicontinuous morphology, have been reported in the LC-coil block copolymers,[12, 13] and interesting relationship between the morphology and the LC phase structure have been discussed. Sänger *et al.*[14] observed the order–order transition from PS spheres above the clearing temperature to the PS cylinders in the nematic phase in the PS-LC-PS triblock copolymer with 12 vol% of the PS blocks. Finkelmann *et al.*[15] and Hammond *et al.*[16] reported the order–order transition followed by the LC phase transition in LC-coil diblock copolymer. We have also studied the similar order–order transition due to the phase transition of LC block in our PS-*b*-poly(*lc*) copolymers.[17] Thus, the order–order transition is observed in the LC block copolymers like in the conventional block copolymers.[18, 19]

To extend such morphological studies, we have treated the binary blends of PS-*b*-poly(*lc*) and homopolystyrene (hPS). In these blend systems, the effect of the molecular weight of the respective homopolymer on the microdomain structures must be taken into account. It has been investingated by Hashimoto *et al.* for given volume fractions of block copolymer in the blends comprising polystyrene-*b*-polyisoprene (PS-*b*-PI) and hPS with various molecular weights.[20–22] When hPS has a relatively lower molecular weight giving $r_s \ll 1$ where $r_s = M_{PS,homo}/M_{PS,block}$, the ratio of number average molecular weight of hPS ($M_{PS,homo}$) to that of corresponding polystyrene segment of block

($M_{PS,block}$), the hPS is uniformly dissolved in the PS microdomain. The swelling of PS segment in PS-*b*-PI expands both the interdomain spacing distance and the distance between the neighboring junctions of block chains at the interface. The resulting asymmetry in the effective volume of PS and PI block chains yields the interface curvature. Hence, the morphology may change from lamellae to cylinders and then to spheres by adding the hPS.[20] It is called "wet-brush" regime. In the case of $r_s \geq 1$, on the other hand, hPS is also soluble in the PS microdomain but it is localized in the middle of the domain to expand only the domain spacing distance.[21] The distance between the neighboring junctions of block chains at the interface is thus unaffected by the hPS so that the type of morphology may not change ("dry-brush" regime). Referring to these basic data in the conventional blend systems,[20–22] in this study we examined the microphase morphologies in the PS-*b*-poly(*lc*)/hPS blends. The effects of the molecular weight of hPS, the weight fraction and the microstructure of poly(*lc*) segment were considered. In some specific blends, we found that the well-defined order–order transition in the morphology takes place on the phase transition of poly(*lc*) segment.

EXPERIMENTAL

PS-*b*-poly(*lc*) block copolymer and three homopolystyrenes were prepared by a sequential anionic living polymerization. Details of synthesis are described elsewhere.[9] The characteristics of these polymers are summarized in Table I. The composition of each segment was finally determined by ^{1}H NMR. M_n and M_w/M_n values were estimated from SEC profile based on the standard polystyrene calibration and ^{1}H NMR. PS-*b*-poly(*lc*) used here is composed of the PS segment with $M_n = 26000$ and poly(*lc*) segment with $M_n = 21000$ (see Table I). Three homopolystyrenes, abbreviated here hPS37, hPS26, and hPS08, have the molecular weights of $M_n = 37000, 26000$, and 8200, respectively. Here, the number following to hPS in the abbreviation is $M_n \times 10^{-3}$.

Table I. Characterization of LC block copolymer and homopolystyrenes

Sample	M_n	M_w/M_n[a]	Weight fraction of LC poly(*lc*) segment	r_s[b]
PS-*b*-poly(*lc*)	47000	1.03	0.45[c]	–
hPS37	37000	1.06	–	1.4
hPS26	26000	1.06	–	1.0
hPS08	8200	1.09	–	0.3

[a]Determined by GPC and ^{1}H NMR. [b]The ratio of M_n of homopolystyrene to M_n of the polystyrene segment in PS-*b*-poly(*lc*). [c]Determined by ^{1}H NMR.

The mixtures of PS-*b*-poly(*lc*) and hPS with weight fractions of LC segment of 35% to 10% were dissolved in tetrahydrofuran with the total polymer concentration of 10 wt%, and cast into the films by slow evaporation of solvent during two or three days at room temperature. The resulting film was completely dried in a vacuum oven at 60°C until a constant weight was attained.

Differential scanning calorimetric (DSC) measurements were carried out with a Perkin–Elmer DSC II at a scanning rate of 2°C min^{-1}. X-Ray measurements were performed by using a Rigaku Denki RU-200BH X-Ray generator with Ni-filtered Cu-K_α radiation. Transmission electron microscopic (TEM) observation was performed with a Hitachi H-500 transmission electron microscope with 75 kV of accelerating voltage. The sample was heated to an isotropic temperature of 150°C in an effort to prevent a thermal prehistory, cooled to a predetermined temperature, and annealed for the proper period. Then, the sample was quenched to the room temperature and cut into ultrathin sections with a thickness around 700–1000 Å by ultramicrotome with a glass knife. The sectioned specimens were stained with the vapor of ruthenium tetraoxide (RuO_4) for 10 min before observation.

RESULTS AND DISCUSSION

Characterization and Thermal Behavior of PS-b-poly(lc) Copolymer

DSC thermograms of the neat PS-*b*-poly(*lc*) are shown in curve a of Figure 1. Two transitions taking place on the LC segment, crystal-SmA at 107°C and SmA-isotropic ones at 126°C, are observed together with the glass transition of PS segment at 90°C. Figure 2 represents the electron micrograph for ultrathin section. It clearly demonstrates the lamellar type of microphase segregation with the LC microdomains appearing dark because of preferential staining of biphenyl moiety and ether linkage groups with RuO_4.[9,13]

Figure 3 shows the temperature dependence of the lamellar spacing, *D*, determined by small-angle X-Ray measurement. The lamellar spacing decreases remarkably through the SmA temperature region. On the other hand, it is relatively constant in the crystal and isotropic phases. The reduction is 25%, which is accountable with the conformational change of the main-chain from an extended form to random coil as schematically illustrated in the insert of Figure 3.[10]
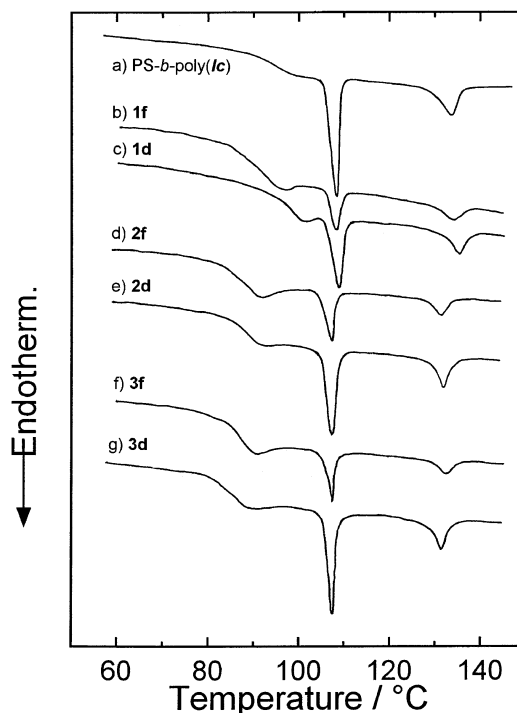

Figure 1. DSC thermograms of the neat block copolymer (curve a) and the blends (curves b–g) measured at a heating rate of 2°C min^{-1}. Two peaks are attributed to the crystal-SmA and SmA-isotropic phase transitions of poly(*lc*) segment.
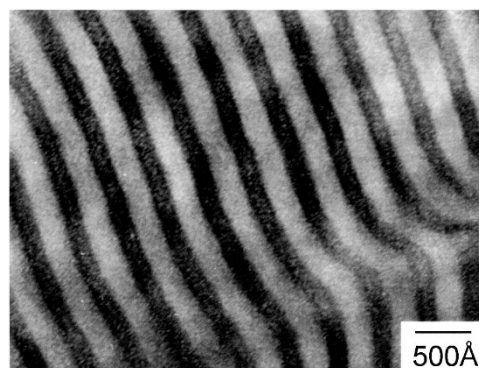

Figure 2. The transmission electron micrograph for the ultrathin section cut out of the neat PS-*b*-poly(*lc*) at crystalline phase stained by RuO_4. This shows a typical lamellar type microphase segregation. Dark area is the LC poly(*lc*) microdomain.

Thermal Behavior of PS-b-poly(lc)/Homopolystyrene Blends

Three blend systems were prepared by blending PS-*b*-poly(*lc*) with three homopolystyrenes, hPS37, hPS26, and hPS08; PS-*b*-poly(*lc*)/hPS37 in blend system **1**, PS-*b*-poly(*lc*)/hPS26 in system **2** and PS-*b*-poly(*lc*)/hPS08 in system **3**. Systems **1**, **2**, and **3**, hence, have the values of r_s = 1.4, 1.0, and 0.3, respectively (see Table I). In each system, we prepared several blend samples with different weight fractions of LC segment; **a** with 35%, **b** with 30%, **c** with 25%, **d** with 20%, **e** with 15%, and **f** with 10%. According to these nota-
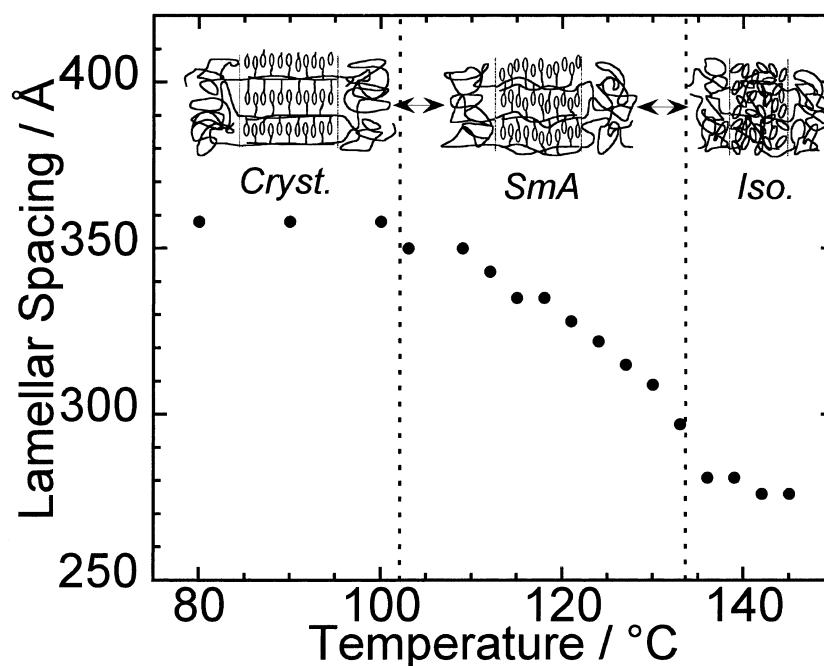
Figure 3. Temperature dependence of the lamellar spacing for neat PS-*b*-poly(*lc*) mesured by small-angle X-Ray scattering. Schematic illustration of the structure changes on Crystal-SmA-Isotropic phase transitions are inserted.

Table II. Characterization of the PS-*b*-ploy(*lc*)/homopolystyrene blends

	Sample	Weight fraction of hPS	Weight fraction of LC segment	Transition temperature/°C (Enthalpy changes/kcal mol^{-1}[a])			
				heating		cooling	
				$T_1(\Delta H_1)$	$T_2(\Delta H_2)$	$T_1(\Delta H_1)$	$T_2(\Delta H_2)$
PS-*b*-poly(*lc*)		–	0.47	108.2 (1.0)	132.6 (0.52)	102.8 (0.99)	133.4 (0.52)
PS-*b*-poly(*lc*)	1a	0.24	0.35	106.8 (0.91)	126.3 (0.50)	101.0 (0.83)	125.4 (0.45)
/hPS37	1b	0.35	0.30	109.3 (0.77)	133.2 (0.38)	103.5 (0.74)	133.2 (0.38)
	1d	0.55	0.20	109.3 (0.75)	135.5 (0.40)	103.5 (0.75)	134.8 (0.44)
	1f	0.78	0.10	108.6 (0.71)	134.1 (0.53)	102.6 (0.62)	133.2 (0.44)
PS-*b*-poly(*lc*)	2a	0.24	0.35	106.8 (0.95)	129.4 (0.54)	101.9 (0.87)	130.7 (0.49)
/hPS26	2b	0.35	0.30	105.5 (0.94)	129.9 (0.45)	99.9 (1.0)	124.0 (0.66)
	2c	0.45	0.25	105.5 (1.1)	125.6 (0.50)	100.1 (1.0)	124.3 (0.67)
	2d	0.55	0.20	107.0 (1.1)	130.0 (0.74)	101.4 (1.1)	129.6 (0.71)
	2e	0.66	0.15	107.0 (1.2)	128.9 (0.62)	101.4 (1.1)	129.1 (0.65)
	2f	0.78	0.10	107.0 (1.1)	128.9 (0.83)	101.4 (1.1)	128.5 (0.71)
PS-*b*-poly(*lc*)	3a	0.24	0.35	106.5 (0.95)	129.1 (0.72)	101.2 (0.89)	128.9 (0.59)
/hPS08	3b	0.35	0.30	107.1 (0.90)	129.9 (0.49)	101.7 (0.90)	130.3 (0.54)
	3c	0.45	0.25	106.6 (0.50)	127.6 (0.50)	101.2 (0.95)	127.4 (0.63)
	3d	0.55	0.20	107.4 (1.1)	129.4 (0.69)	101.8 (1.0)	129.1 (0.66)
	3e	0.66	0.15	107.7 (1.1)	130.5 (0.62)	102.1 (1.1)	129.3 (0.53)
	3f	0.78	0.10	108.3 (0.93)	132.3 (0.83)	102.5 (0.90)	131.6 (0.71)

[a] Estimated per mole of LC poly(*lc*) segment.

tions, the blend samples were named as **Xy** where **X** is the system number (**1**–**3**) and **y** is the alphabet (**a**–**f**) showing the weight fraction of LC segment (refer to Table II).

Typical DSC thermograms of blend samples are shown in curves b–g of Figure 1. All blends exhibit the two phase transitions similarly as PS-*b*-poly(*lc*).[9, 10] The phase sequence is also similar; the crystal-SmA and SmA-isotropic phase transitions take place. The transition temperatures and enthalpies are summarized in Table II. We can again find that the values of transition temperature and enthalpies are similar to those of the neat PS-*b*-poly(*lc*). Hence, it is concluded that the crystallinity and liquid crystallinity of the poly(*lc*) segment in its microdomain are not essentially affected by mixing the hPS.
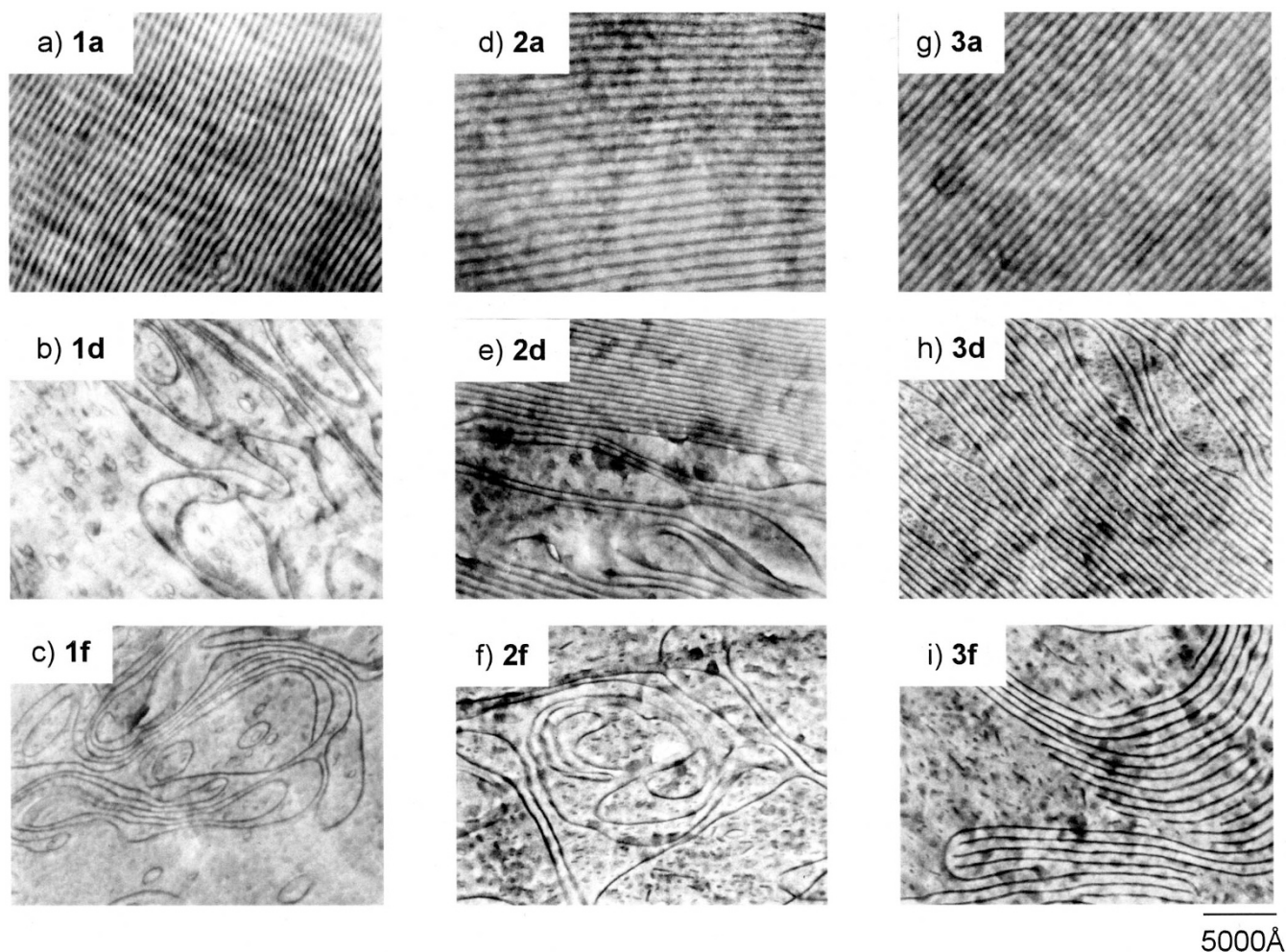
Figure 4. Transmission electron micrographs for the ultrathin section cut out of PS-*b*-poly(*lc*)/hPS blends at crystalline phase; **1a**, **1d**, and **1f** in system **1**, **2a**, **2d**, and **2f** in system **2**, and **3a**, **3d**, and **3f** in system **3**.

TEM and SAXS Measurements of PS-b-poly(lc)/Homopolystyrene Blends

Morphology in Crystalline Temperature Region of LC Segment. Figure 4 shows electron micrographs for ultrathin sections cut out of the PS-*b*-poly(*lc*)/hPS blends. Here, the blend samples were initially heated up to the isotropic phase at 140°C, cooled down to the liquid crystalline phase at 115°C at a rate of 0.1°C min^{-1}, and annealed for 1 week. Then, they were again cooled to the crystalline phase at a rate of 0.1°C min^{-1}. By such a careful treatment, the LC segment in its microdomain is believed to be well crystallized.

As found in Figure 4, no macroscopic phase separation is involved for all blends with the crystal poly(*lc*) segment. It is further found that the hPS dose not significantly perturb the long-range spatial order of the lamellar microdomains. The expansion in the inter-lamellar spacing causes undulation of the lamellae or bending of the interface resulting in a broader distribution of the spacing between lamellae. Its most typical example can be seen in the micrographs of **1d** and **1f**. According to Hashimoto's work for PS-*b*-PI/hPS,[22]

the blends in a system **1** with r_s = 1.4 are evidently classified into the "dry-brush" regime. Hence, it is expected that the hPS does not expand the distance between the neighboring junctions of PS-*b*-poly(*lc*) at the interface, but the interdomain distance by locating in the middle of the PS domain. Thus, the observation is reasonable that the lamellar morphology in a series of **1** is strongly sustained with the variation of hPS content. On the other hand, some small pieces of lamellae coexist with long ranged lamellae in system **3** which is surely in the "wet-brush" regime, but the situation is essentially similar to that in system **1**. In the crystalline phase, thus, the hPS, even if it has the lower molecular weight, doesn't expand seriously the distance between the neighboring junctions at the interface.

When the content of hPS is relatively lower, the lamellar packing is somewhat regular enough to allow the estimation of the lamellar spacing by the small angle X-Ray method. The lamellar sapcings, *D*, are listed for **1a**, **2a**, **2b**, **3a**, and **3b** in Table III, and are compared with the calculated values under the assumption of the perfect "dry brush". *D* for **1a** is almost equal
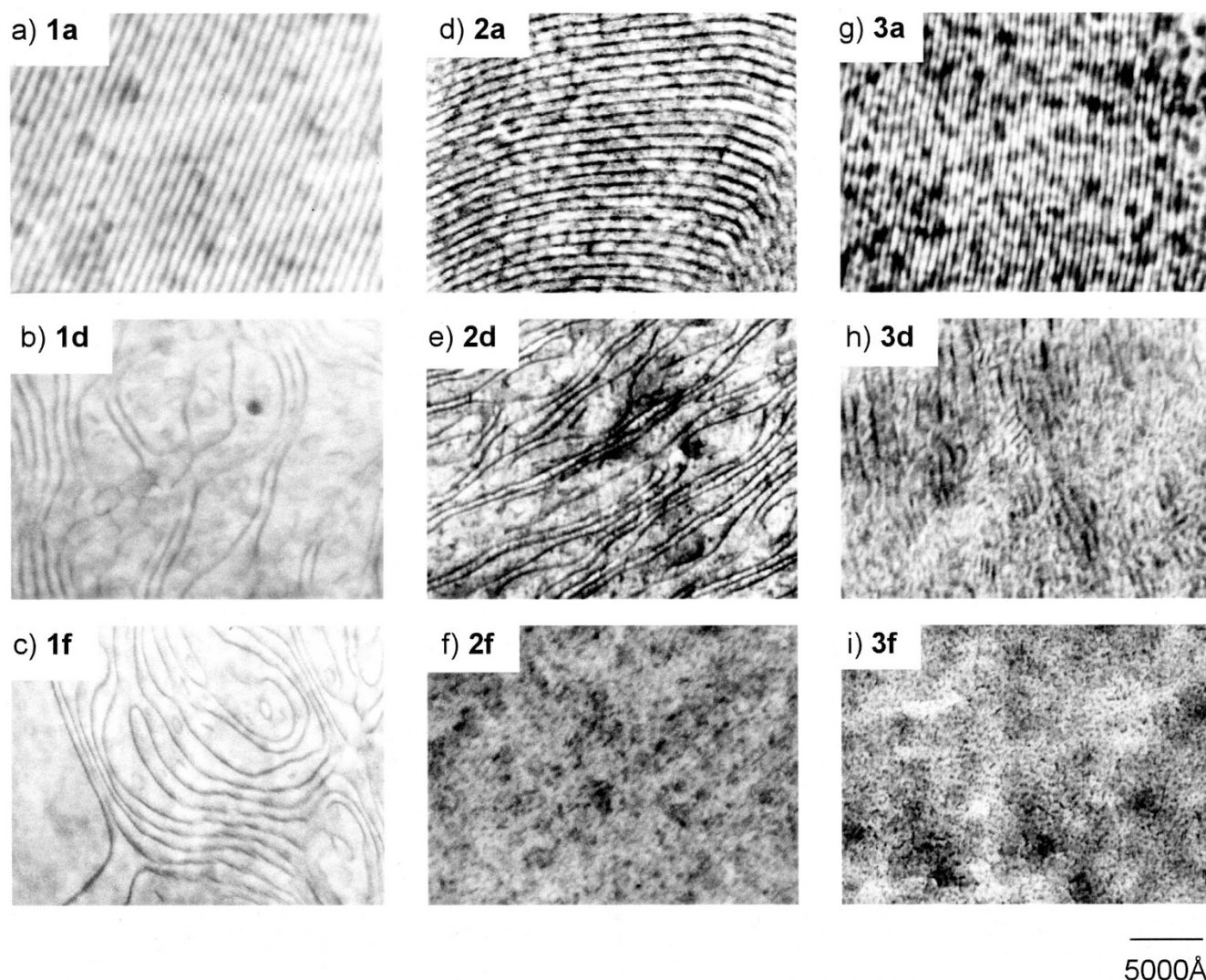
Figure 5. Transmission electron micrographs for the ultrathin section cut out of PS-*b*-poly(*lc*)/hPS blends which were quenched from the isotropic phase at 140°C after annealing for 24 h; **1a**, **1d**, and **1f** in system **1**, **2a**, **2d**, and **2f** in system **2**, and **3a**, **3d**, and **3f** in system **3**.

Table III. Lamellar spacing of PS-*b*-poly(*lc*)/homopolystyrene blends

	$D_{obs.}$/Å	$D_{calc.}$/Å[a]
1a	442	442
2a	434	442
2b	490	517
3a	418	442
3b	470	417

[a]Calculated by assuming "dry brush" regime (see the text).

to the calculated one, but D for **3a** and **3b** are relatively smaller than the calculated values, implying that the hPS08 expands somewhat the distance between the neighboring chains of PS-*b*-poly(*lc*) at the interface of the microdomain although the degree of expansion is not so large.

Thus, it seems that all the systems in a crystalline phase behave as in a "dry-brush" regime irrespective of the molecular weight of hPS blended.

Morphology in Isotropic Temperature Region of LC

Segment. Next, we tried to examine the morphology in the isotropic temperature region of LC segment. For this purpose, the materials were heated to 140°C, annealed for 24 h, and then quenched to room temperature. Figure 5 shows the TEM photographs for the same materials as presented in Figure 4. By comparing Figures 4 and 5, one knows that for any blends in system **1** the lamellar morphology is similarly observed as in the crystalline phase. On the other hand, in some blends of systems **2** and **3**, the morphology is drastically altered. The typical change can be seen in **2f** and **3f** where only the spherical microdomain can be seen. From a series of photographs in system **3**, the morphology is found to depend on the content of PS so that the lamellar microdomain in **3a** is altered to the cylinder-like domain in **3d** and finally to the sphere domain in **3f** with the increase of the content of PS. This is just expected for the blends in the "wet-brush" regime; the low molecular weight hPS08 can swell the PS domain of block copolymer and spread the distance between the neigh-
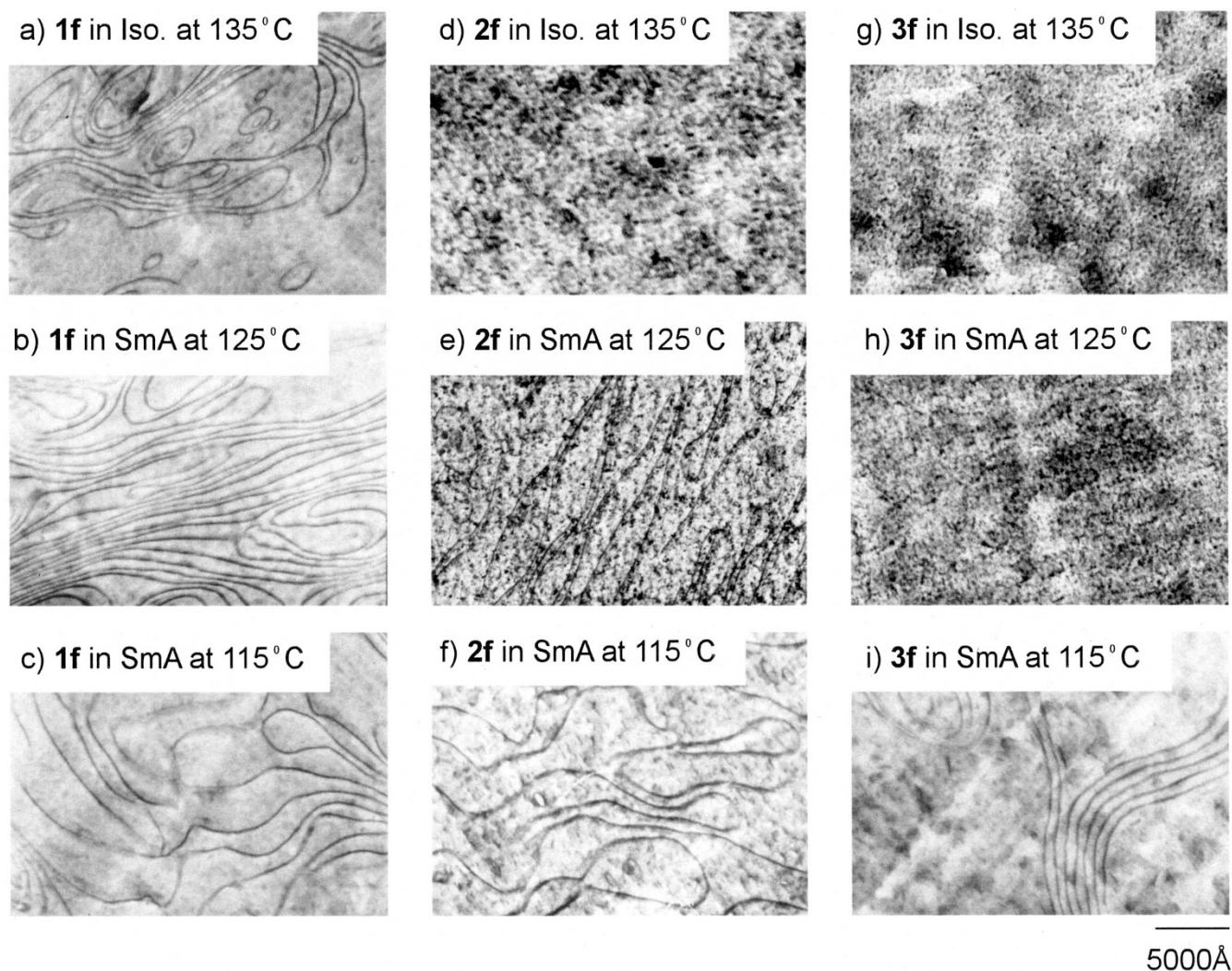
Figure 6. Transmission electron micrographs of **1f**, **2f**, and **3f** which were quenched from the SmA phase at 115°C, the SmA phase at 125°C and the isotropic phase at 135°C, respectively.

boring chains at the interface of the microdomain of the block copolymer to yield the interface curvature of the cylinder or sphere microdomain.

Morphological Changes on Phase Transition of LC Segment. By comparing the microphotographs of **3f** in Figures 4 and 5, one can realize that the morphology in blends strongly depends on the phase structure of the poly(*lc*) segment.[12, 13] To clarify the order–order transition expected, the blend samples were annealed at respective temperatures; at 135°C (isotropic temperature) for 24 h, at 125°C (LC temperature near the isotropization temperature) for 1 week, and at 115°C (LC temperature region near the crystallization temperature) for 1 week. All the annealed samples were then quenched to room temperature. Figure 6 represents the typical micrographs observed for **1f**, **2f**, and **3f**.

1f sustains to form the lamellar microdomain over the whole temperature region as expected from the data in Figures 4 and 5. In **2f** the spherical microdomain of the isotropic phase is altered to lamellar microdomain

on the transition to the LC phase. In **3f**, spherical microdomain can be seen in the LC phase at 125°C as well as in the isotropic phase, and transforms to the lamellar microdomain in the LC phase at lower temperatures. Thus, the order–order transition is likely to take place when both the molecular weight of hPS blended and the weight fraction of LC segment are relatively lower. The order–order transitions observed in system **3** are schematically illustrated as functions of the temperature and the fraction of LC segment in Figure 7b. This result is interestingly compared with that of Figure 7a, as observed for system **1**, where the lamellar microdomain is invariably formed in the whole region of temperature and LC content.

The order–order transition typically observed for the blends of system **3** with the lower weight fraction of LC segment, for example **3d**, **3e**, and **3f**, can be understood as following. At the isotropic temperatures, the hPS08 with $r_s = 0.3$ spreads strongly the distance between the neighboring chains at the interface of the mi-
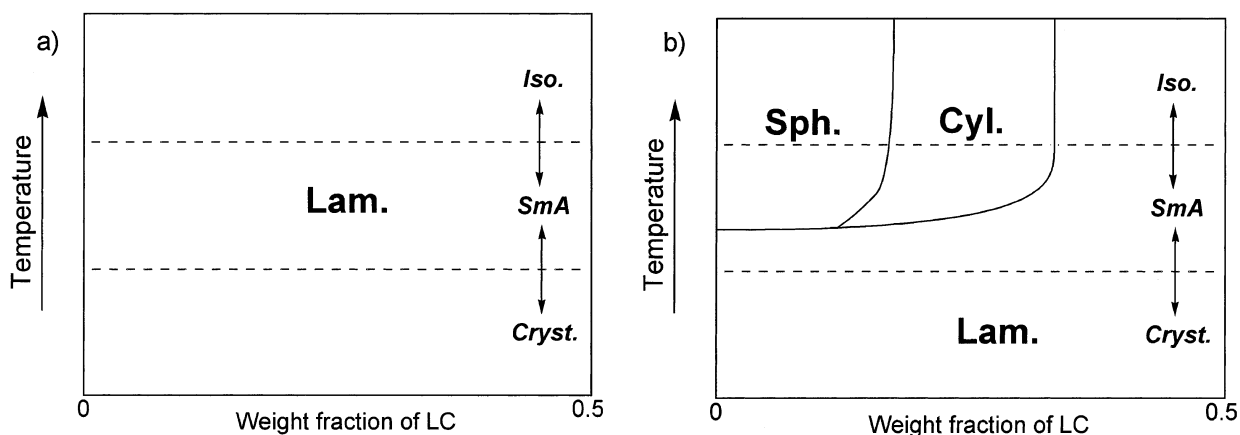
Figure 7. Variation of the microphase structures with the temperature and weight fraction of LC segment: a) in system **1** and b) in system **3**.
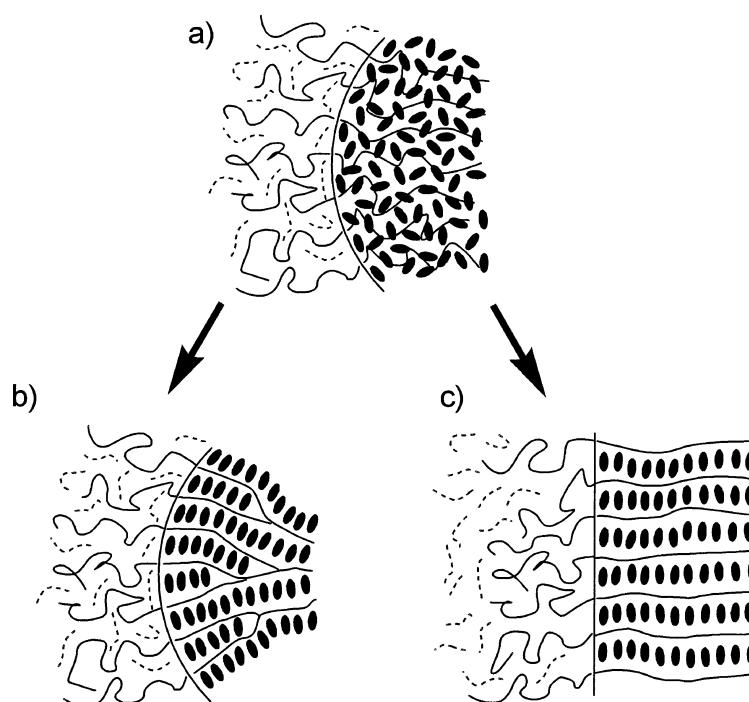

Figure 8. Schematical illustration of the microphase structure varying with the phase structure of LC segment: a) isotropic phase in spherical microdomain, b) SmA in spherical microdomain, and c) SmA in lamellar microdomain.

crodomain of the PS-*b*-poly(*lc*) because of the preferred swelling into the PS microdomain. This results in the morphological change from lamella of the neat block to cylinder or sphere (refer to Figure 8a). On transition to the liquid crystalline phase of the LC segment, the side-chain mesogens take up the uniaxial orientation to form the smectic layer, simultaneously the main-chain of the poly(*lc*) segment changes from the random coil to the extended form, and then the smectic layers are formed perpendicularly to the interface.[10] Considering that the radius of sphere or cylinder is around 200–300 Å which is roughly ten times as large as the smectic layer thickness of 26 Å, the smectic layers developing from the largely curved interface cannot be packed effectively without layer deformation (see Figure 8b).

Only the flat interface from the lamellar microdomains is comfortable for the smectic or crystal layer structure (Figure 8c). Thus, in LC phase at lower temperatures or in the crystalline phase, the lamellar domain is preferred by overcoming the entropy loss due to exclusion of homopolystyrene from the polystyrene microdomain of block copolymer.

CONCLUSION

The interrelationship between the microdomain structure and the thermotropic phase structure of LC segment was studied in LC-coil block copolymer (PS-*b*-poly(*lc*))/homopolystyrene (hPS) blend samples. Neat block and all the blends with various composi-

tions of LC content from 35% to 10% exhibited the well-defined microphase segregation and the LC segment in its microdomain underwent the well defined crystal-SmA-isotropic transitions. The hPS is thus soluble into the PS domain of the LC block copolymer.

The microdomain structure depends on both the molecular weight of homopolystyrene blended and the phase structure of LC segment. When the highest molecular weight polystyrene with M_n = 37000 was blended (so called in a "dry-brush" regime), a lamellar type of morphology was observed invariably even if the composition and temperature are varied. In contrast, when the lowest molecular weight polystyrene with M_n = 8200 was used (in a "wet-brush" regime), the type of morphology was significantly varied. At the isotropic temperatures of LC segment, the lamellar morphology was observed for the blends with LC contents from 45% to 35%, but the cylinder or sphere domain appeared with a decrease in the LC content. On the other hand, at the crystal temperatures or at the lower SmA temperatures, the lamellar morphology was commonly formed. In some blends with the lower weight fractions of LC segment of 10% to 30%, hence, there was seen the order–order transition from sphere or cylinder to lamella on decreasing the temperature from isotropic to crystal phase. This morphological change is caused by the formation of the layered structure that tends to orient perpendicularly to the interface of microdomain, leading to the reasonable conclusion that both the microdomain morphology and the solubility style of the homopolymer are dominated by the counterbalance between the energy gain due to the layer formation of LC segment and entropy loss due to the exclusion of the hPS from the microdomain of the PS segment.

REFERENCES

1. J. Adams and W. Gronski, *Makromol., Chem., Rapid Commun.*, **10**, 553 (1989).

2. M. Walther and H. Finkelmann, *Prog. Polym. Sci.*, **21**, 951 (1996).
3. G. Mao and C. K. Ober, *Acta Polym.*, **48**, 405 (1997).
4. S. Poser, H. Fischer, and M. Arnold, *Prog. Polym. Sci.*, **23**, 1337 (1998).
5. G. Mao, J. Wang, C. K. Ober, M. Brehmer, M. J. O'Rourke, and E. L. Thomas, *Chem. Mater.*, **10**, 1538 (1998).
6. A. Moment, R. Miranda, and P. T. Hammond, *Macromol. Rapid Commun.*, **19**, 573 (1998).
7. J. F. Gohy, S. Antoun, R. Sobry, G. V. Bossche, and R. Jérôme, *Macromol. Chem. Phys.*, **201**, 31 (2000).
8. O. Lehmann, S. Förster, and J. Springer, *Macromol. Rapid Commun.*, **21**, 133 (2000).
9. M. Yamada, T. Iguchi, A. Hirao, S. Nakahama, and J. Watanabe, *Macromolecules,* **28**, 2556 (1995).
10. M. Yamada, T. Iguchi, A. Hirao, S. Nakahama, and J. Watanabe, *Polymer J.*, **30**, 23 (1998).
11. M. Yamada, T. Itoh, A. Hirao, S. Nakahama, and J. Watanabe, *High Perform. Polym.*, **10**, 131 (1998).
12. G. Mao, J. Wang, S. R. Clingman, C. K. Ober, J. T. Chen, and E. L. Thomas, *Macromolecules,* **30**, 2556 (1997).
13. M. Yamada, T. Itoh, R. Nakagawa, A. Hirao, S. Nakahama, and J. Watanabe, *Macromolecules,* **32**, 282 (1999).
14. J. Sänger, W. Gronski, S. Maas, B. Stühn, and B. Heck, *Macromolecules,* **30**, 6783 (1997).
15. A. Schneider, J. J. Zanna, M. Yamada, H. Finkelmann, and R. Thomann, *Macromolecules,* **33**, 649 (2000).
16. M. Anthamatten and P. T. Hammond, *Macromolecules,* **32**, 8066 (1999).
17. T. Itoh, M. Yamada, A. Hirao, S. Nakahama, and J. Watanabe, *Mol. Cryst. Liq. Cryst.*, **347**, 211 (2000).
18. L. Leibler, *Macromolecules,* **13**, 1602 (1980).
19. S.Sakurai, H. Hasegawa, T. Hashimoto, and L. J. Fetters, *Macromolecules*, **26**, 5796 (1993).
20. T. Hashimoto, H. Tanaka, and H. Hasegawa, *Macromolecules,* **23**, 4378 (1990).
21. S. Koizumi, H. Hasegawa, and T. Hashimoto, *Makromol. Chem., Macromol. Symp.*, **62**, 75 (1992).
22. H. Hasegawa and T. Hashimoto, 'Self-Assembly and Morphology of Block Copolymer Systems' in "Comprehensive Polymer Science, Suppl. 2," S. L. Aggarwal and S. Russo Ed., Pergamon, Oxford, 1996, p 497.